UNIVERSITY OF WATERLOO
UNIVERSITY OF WATERLOO
UNIVERSITY OF WATERLOO

COMPUTER SCIENCE DEPARTMENT
COMPUTER SCIENCE DEPARTMENT
COMPUTER SCIENCE DEPARTMENT

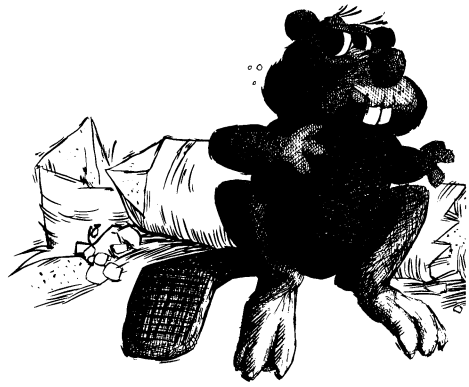

Simulation of Nonaqueous Phase Groundwater Contamination

Research Report

Peter A. Forsyth

CS-88-02

February, 1988

Simulation of Nonaqueous Phase Groundwater Contamination

Peter A. Forsyth

Department of Computer Science
University of Waterloo
Waterloo, Ontario
N2L 3G1

ABSTRACT

Simulation of groundwater contamination by nonaqueous phase contaminants requires solution of the multiphase flow equations for a porous medium. A three phase, two dimensional, two component (water, contaminant) model is developed. The contaminant can partition between the air, water and nonaqueous phase. An adaptive implicit method is used to discretize the equations. In order to rigorously solve the flow and constraint equations in cells where the nonaqueous phase saturation is identically zero, a variable substitution method is used. A detailed discussion of the boundary conditions is also presented.

1. Introduction

Recently, there has been considerable interest in modelling of groundwater contamination by nearly immiscible fluids. Some examples of this type of contamination are fuel oil and gasoline leakage from underground storage tanks, and leaching of hazardous organic chemicals from toxic waste dumps. Since these contaminants are only slightly water soluble, these systems can be simulated on the basis of the multi-phase flow equations for a porous medium [1]. Several authors [2-8] have proposed various

formulations for solving these problems. As pointed out by Abriola and Pinder [6], the equations of multiphase contaminant flow are highly non-linear, and stability requirements necessitate some form of implicit treatment. This makes these simulations extremely CPU intensive.

The purpose of this article is to apply some recently developed numerical methods to the solution of multiphase groundwater contaminant problems. Three phase, two component, two dimensional systems with mass transfer between the phases will be considered. An adaptive implicit method [9] will be used to discretize the flow equations. This technique can result in considerable savings over a fully implicit method, while allowing timestep sizes comparable to a fully implicit method. To avoid the problem of having to specify a small amount of the contaminant phase everywhere [5], a variable substitution method will be used to account for phase appearance and disappearance. The results for some example simulations will be given, and comparisons with some previously published results, where available, are also included.

2. Formulation

In reality, a groundwater - contaminant system consists of three components: air, water and contaminant. However, in shallow groundwater systems, it is common practice to ignore the convective movement of the air phase, [2,6] and to assume that the air phase pressure is constant. This assumption allows neglect of the air mass balance equation, thus reducing the number of equations and unknowns by one. This approximation has been shown to be reasonable as long as the relative permeability to air near the critical air saturation is not too flat, and the air-water capillary pressure is not too small [10]. The air phase is still taken into account, however, in its affect on three phase relative permeability, and

diffusional transport of the contaminant.

A single component contaminant will be considered. This contaminant can partition between the air, water and non-aqueous phases. Convective transport of the contaminant can occur both in the water and non-aqueous phases, while diffusive transport can occur only in the air phase. These assumptions were also used in [4,5,6]. Some recent computations for one dimensional systems with an immovable non-aqueous phase have demonstrated that for realistic values of the physical parameters, the diffusive and dispersive movement of contaminant in the water phase is small compared with diffusive transport in the air phase [7], and hence can be ignored. Abriola and Pinder [5] also noted that contaminant plumes in the water phase were due primarily to gas phase diffusion and local phase equilibrium. Consequently, the diffusive and dispersive transport of contaminant in the water phase will be ignored in the following. However, the numerical techniques used in this paper do not in any way require this assumption.

In common with previous authors, it will also be assumed that the dissolved contaminant does not affect the fluid properties of the water-phase. Recalling that the air phase pressure is assumed constant, the equations for three phase air (a), water (w) and non aqueous (n) contaminant transport are:

Water mass balance:

$$\frac{\partial}{\partial t}(\phi \rho_w S_w) = q_w \tag{1}$$

$$+ \nabla \cdot \left[\frac{K \rho_w K_{rw}}{\mu_w} (\nabla P_w - \rho_w g \nabla D) \right]$$

Contaminant mass balance:

$$\frac{\partial}{\partial t}\left(\phi\rho_n S_n + C_n^a \phi S_a + C_n^w \phi S_w\right) \tag{2}$$

$$= q_n + \frac{C_n^w}{\rho_w} q_w + \frac{C_n^a}{\rho_a} q_a$$

$$+ \nabla\cdot\left[\frac{K\rho_n K_{rn}}{\mu_n}\left(\nabla P_n - \rho_n g \nabla D\right)\right]$$

$$+ \nabla\cdot\left[\frac{K C_n^w K_{rw}}{\mu_w}\left(\nabla P_w - \rho_w \nabla D\right)\right]$$

$$+ \nabla\cdot\left[\phi S_a D_r^a \xi_a \nabla C_n^a\right]$$

where:

ϕ	=	porosity
ρ_ℓ	=	density of phase $\ell = a, w, n$ (M/L^3)
S_ℓ	=	saturation of phase ℓ
q_ℓ	=	source/sink term for phase ℓ (M/T)
K	=	absolute permeability (L^2)
μ_ℓ	=	dynamic viscosity of phase ℓ (M/LT)
$K_{r\ell}$	=	relative permeability of phase ℓ
P_ℓ	=	pressure of phase ℓ (M/LT^2)
g	=	gravitational acceleration (L/T^2)
D	=	depth (L)
C_n^ℓ	=	concentration of contaminant in phase ℓ (M/L^3)
D_n^a	=	molecular diffusion constant for contaminant in the air phase (L^2/T)
ξ_a	=	air phase tortuosity factor
q_ℓ	=	source term for phase ℓ (M/T)

In addition, to the above equations which describe the flow of fluids, there are additional relationships among the variables. For example, the saturations sum to one:

$$S_n + S_w + S_a = 1 \tag{3}$$

The phase pressures are related through the capillary pressures, which are experimentally determined functions of the saturations:

$$P_a - P_n = P_{can}\ (S_a) \tag{4}$$

$$P_n - P_w = P_{cnw}\ (S_w) \tag{5}$$

Note that the assumption of constant P_a effectively gives S_a as a function of P_n from equation (4). A discussion of the methods for modelling saturated-unsaturated flow is given in [10].

The relative permeabilities of the water - *NAPL* (non-aqueous phase liquid) are determined experimentally, as are the relative permeabilities for the air-nonaqueous phase system [11]. The three phase *NAPL* relative permeability is obtained using Stone's second method [2,12,13]. Viscosities and densities are assumed constant, while the porosity has the form:

$$\phi = \phi_o\ [1 + C_f\ (P_n - P_o)] \tag{6}$$

where ϕ_o is the porosity at $P_n = P_o$. Assuming the presence of *NAPL*, the concentrations of the contaminant in the air and water phases are:

$$C_n^a = K_n^a \tag{7}$$

$$C_n^w = K_n^w$$

where K_n^ℓ are the partition coefficients. However, if the *NAPL* phase is not present, equations (7) must be modified. This will be discussed in a later Section. A detailed description of the physical

assumptions involved in the above model is given in references [4,5,6]. A description of multicomponent phase behaviour is given in [7,8].

The above equations are discretized using a cell centered finite difference scheme, similiar to that used previously [2,4,5]. A conservative difference scheme with upstream weighting of the mobilities is used. The discretized equations are:

Water equation:

$$\frac{V_i}{\Delta t}\left[(\phi S_w \rho_w)_i^{N+1} - (\phi S_w \rho_w)_i^N\right] - q_w^{N+1} \tag{8}$$

$$-\frac{V_i}{\Delta x_i}\left[T_{w,i+\frac{1}{2}}^M \rho_{n,i+\frac{1}{2}}^M K_{i+\frac{1}{2}} \psi_{w,i+\frac{1}{2}} - T_{w,i-\frac{1}{2}}^M \rho_{i-\frac{1}{2}}^M K_{i-\frac{1}{2}} \psi_{w,i-\frac{1}{2}}\right]$$

$$+ (y \text{ terms}) = 0$$

Contaminant equation

$$\frac{V_i}{\Delta t}\left[(\phi\rho_n S_n)_i^{N+1} - (\phi\rho_n S_n)_i^N + (C_n^a \phi S_a)_i^{N+1} - (C_n^a \phi S_a)_i^N\right. \tag{9}$$

$$\left. + (C_n^w \phi S_w)_i^{N+1} - (C_n^w \phi S_w)_i^N\right]$$

$$- q_n^{N+1} - \left(\frac{C_n^w q_w}{\rho_w}\right)^{N+1} - \left(\frac{C_n^a q_a}{\rho_a}\right)^{N+1}$$

$$- \frac{V_i}{\Delta x_i}\left[T_{n,i+\frac{1}{2}}^M \rho_{n,i+\frac{1}{2}}^M K_{i+\frac{1}{2}} \psi_{n,i+\frac{1}{2}} - T_{n,i-\frac{1}{2}}^M \rho_{n,i-\frac{1}{2}}^M K_{i-\frac{1}{2}} \psi_{n,i-\frac{1}{2}}\right]$$

$$- \frac{V_i}{\Delta x_i}\left[(C_n^w T_w)_{i+\frac{1}{2}}^M K_{i+\frac{1}{2}} \psi_{w,i+\frac{1}{2}} - (C_n^w T_w)_{i-\frac{1}{2}}^M K_{i-\frac{1}{2}} \psi_{w,i-\frac{1}{2}}\right]$$

$$-\frac{V_i}{\Delta x_i}\left[(\phi\, S_a\, D_n^a\, \xi_a)_{i+\frac{1}{2}}^M \left\{\frac{(C_n^a)_{i+1}^M - (C_n^a)_i^M}{(\Delta x_i + \Delta x_{i+1})/2}\right\}\right.$$

$$\left. + (\phi S_a\, D_n^a \xi_a)_{i-\frac{1}{2}}^M \left\{\frac{(C_n^a)_{i-1}^M - (C_n^a)_i^M}{(\Delta x_i + \Delta x_{i-1})/2}\right\}\right]$$

$$+ (y \text{ terms}) = 0$$

In the above, the subscript i refers to the i'th finite difference cell, V_i is the volume of the i'th cell. The mobilities T_ℓ are defined by:

$$T_\ell = \frac{K_{r\ell}}{\mu_\ell}$$

$T_{\ell\, i+\frac{1}{2}}$ represents either $T_{\ell,i}$ or $T_{\ell,i+1}$ depending on which is the upstream point for phase ℓ. Upstream weighting is also used for the term:

$$(C_n^w\, T_w)_{i+\frac{1}{2}}$$

The absolute permeability is defined using the harmonic mean [2]. The effective diffusion coefficient:

$$(\phi\, S_a\, D_n^a \xi_a)_{i+\frac{1}{2}}$$

is also defined harmonically. The superscripts N or $N+1$ refer to the time level. M can be either N or $N+1$ depending on the adaptive implicit state of cell i.

The potential terms ψ are given by:

$$\psi_{n,i+\frac{1}{2}} = (P_{n,i+1}^{N+1} - P_{n,i}^{N+1})/\Delta x_{i+\frac{1}{2}} - \rho_{n,i+\frac{1}{2}}^M\, g\,(D_{i+1} - D_i)/\Delta x_{i+\frac{1}{2}} \tag{10}$$

$$\psi_{w,i+\frac{1}{2}} = (P^{N+1}_{n,i+1} - P^{N+1}_{n,i})/\Delta x_{i+\frac{1}{2}}$$
$$- (P^{N+1}_{cnw,i+1} - P^{N+1}_{cnw,i})/\Delta x_{i+\frac{1}{2}}$$
$$- \rho^{M}_{w,i+\frac{1}{2}}\, g\,(D_{i+1} - D_i)/\Delta x_{i+\frac{1}{2}}$$

$$\Delta x_{i+\frac{1}{2}} = (\Delta x_i + \Delta x_{i+1})/2$$

The convergence properties of such difference approximations on irregular cell centered grids is given elsewhere [14].

When $M=N$ in equations (9-10), the discretization is similar to the *IMPES* (implicit pressure, explicit saturation) method used in petroleum reservoir simulation [1]. When $M=N+1$, the discretization is fully implicit. The adaptive implicit method [9,15] attempts to minimize computational work by using a fully implicit method in those regions undergoing large flows, while using an *IMPES* method elsewhere. A discussion of the switching strategy will be given in a following section.

The discretized equations (9) are solved using full Newton iteration.

3. Variable Substitution

If S_n is non-zero, then equations (9-10) with constraint equation (7) can be formally solved for the two primary variables $P^{N+1}_{n,i}$, $S^{N+1}_{w,i}$ by full Newton iteration. All other variables are functions of these unknowns.

However, if $S_{n,i} = 0$, then equation (7) no longer applies. This problem was avoided previously [5] by defining a "pseudo K value", K' such that:

$$(K_n^w)' = \left(\frac{S_n}{S_n + 10^{-4}} \right) K_n^w \tag{11}$$

$$(K_n^a)' = \left(\frac{S_n}{S_n + 10^{-4}} \right) K_n^a$$

and specifying a small non-zero S_n everywhere. Equation (11) prevents complete disappearance of the nonaqueous phase since complete vaporization or solubization of the contaminant is prohibited. This "pseudo K" value method has been used in reservoir simulation, but can require very small tolerances to achieve good material balance errors [16].

A more rigorous approach uses variable substitution. Consider a cell with $S_{n,i} > 0$, then the primary variables are:

$$P_{n,i} \ , \ S_{w,i}$$

with

$$C_{n,i}^w = K_n^w$$

$$C_{n,i}^a = K_n^a$$

If any Newton iteration produces an $S_{n,i} < 0$, then the primary variables are switched to:

$$P_{n,i} \ , \ C_{n,i}^w \tag{12}$$

with constraints:

$$S_{n,i} = 0 \tag{13}$$

$$C^a_{n,i} = \left(\frac{K^a_n}{K^w_n}\right) C^w_{n,i}$$

If the independent variables are $P_{n,i}$, $C^w_{n,i}$ and any Newton iteration produces a $C^w_{n,i}$ such that:

$$C^w_{n,i} > K^w_n \tag{14}$$

then the independent variables are switched back to $P_{n,i}$, $S_{w,i}$. This approach allows the nonaqueous phase saturation to be identically zero. Note that generally $S_n \equiv 0$ everywhere at the beginning of a simulation.

If K^w_n was identically zero in the above example, then C^a_n would be used as a primary variable. If both K^w_n, K^a_n are identically zero, then variable substitution is suppressed, with the independent variables being P_n, S_w. In regions where $S_{n,i} = 0$, then equation (2) merely states that $0 = 0$. However, this equation does posess derivatives with respect to $S_{w,i}$ (recall equations (3-4)), so that the Jacobian is nonsingular.

4. The Adaptive Implicit Method

As mentioned earlier, the basic idea behind an adaptive implicit method is to use a fully implicit technique only in those regions where required ($M=N+1$ in equations (8-9)), while using an explicit method ($M=N$) elsewhere. Note that even if $M=N$, the pressure P_n is still taken implicitly in the flow terms, and hence couples nearest neighbour cells. By analogy with petroleum reservoir simulation, cells with $M=N$ will be refered to as *IMPES* cells (implicit pressure, explicit saturation). Clearly, if there are large regions where an *IMPES* method is stable, then significant savings in computational work will result. In particular, it is

expected that those regions where $S_{n,i}=0$ can be solved using an *IMPES* method in many cases.

The discretized equations (8-9) are solved using full Newton iteration, and the Jacobian is solved using an incomplete *LU* iterative solver with *ORTHOMIN* acceleration [9,17,18,19]. Note that even if $M=N$, all variables occur at $t=N+1$ in the mass accumulation term. Elementary matrix operations are required to decouple *IMPES* variables from the Jacobian. Full details concerning the construction of the Jacobian, decoupling of the *IMPES* unknowns, and the matrix solve are given in [9].

When $P_{n,i}$ and $S_{w,i}$ are independent variables, equations (1-2) are too complex to allow a reasonable stability analysis, especially in the case of multi-dimensional flows. Note that only recently has a stability analysis been carried out for one dimensional, two phase incompressible flows with gravity but no capillary pressure [20]. This work has recently been extended to include capillary pressure [21], but this is a long way from being applicable to three phase, multidimensional systems. Consequently, the conservative switching strategy used in reference [9] will be used here. Only switching from *IMPES* to fully implicit is allowed. The switching occurs when the saturation change exceeds a small fraction (typically 25%) of the timestep selector norm [9]. Switching can occur after any Newton iteration.

On the other hand, when P_n C_n^w are primary variables, it is possible to analyse the stability of equations (8-9) if a few simplifying assumptions are made. The stability criteria in this case are given in the Appendix, and are used to switch from *IMPES* to fully implicit if C_n^w is a primary variable.

5. Boundary Conditions

The system of equations (1-2) has both hyperbolic and parabolic properties. The pressure can be considered to be a parabolic-like variable, while the saturation or concentration is a hyperbolic-like variable. All physically possible boundary conditions can be specified by forcing no - flow at all boundaries, and using source/sink terms to simulate injection and production of fluids. For example, an aquifer can be modelled by specifying an injection/production rate which forces a constant pressure ($P_w = P_w^*$) boundary. For brevity, the subscript i will be dropped in the following. Unless otherwise noted, all unsubscripted variables refer to qualities evaluated in the i'th cell. Consequently, an aquifer boundary with $P_w = P_w^*$ is specified by :

$$q_w = \frac{K K_{rw}}{\mu_w} \rho_w W_i (P_w^* - P_w); \qquad (P_w^* - P_w) < 0 \tag{15}$$

$$= \frac{K K_{rw}(S_w=1)}{\mu_w} \rho_w W_i (P_w^* - P_w); \qquad (P_w^* - P_w) > 0$$

$$q_n = \frac{K K_{rn} \rho_n W_i}{\mu_n} (P_n^* - P_n) + \min\left(0, \frac{C_n^w q_w}{\rho_w}\right); \qquad (P_n^* - P_n) < 0$$

$$= 0 \qquad ; \qquad (P_n^* - P_n) > 0$$

where:

$$P_n^* = P_w^* + P_{cnw}(S_w=1)$$

and where W_i is a large number selected so that:

$$P_w^* - P_w << P_w^*$$

On the other hand, if an air boundary is to be modelled, then a

constant air pressure $P_a = P_a^*$ can be specified. If $P_n < P_a^*$, then no fluid flow (either water or *NAPL*) can take place across the boundary.

Consequently:

$$q_w = 0 \tag{16}$$

$$q_n = -S_a W_i C_n^a ; \quad P_n < P_a$$

Where W_i is again selected so that:

$$| S_a C_n^a | < \epsilon ; \quad \epsilon << 1$$

The above conditions have the effect of forcing $C_n^a = 0$ on the boundary. This assumes that there is instantaneous equilibrium between the air phase at the boundary of the porous medium and the air phase at the surface.

$$\text{If} \quad P_n > P_a^* , \quad \text{then:} \tag{17}$$

$$q_w = \frac{K K_{rw} \rho_w}{\mu_w} (P_a^* - P_w); \qquad (P_a^* - P_w) < 0$$

$$= 0 \qquad ; \qquad (P_a^* - P_w) > 0$$

$$q_n = \frac{K K_{rn} \rho_n W_i}{\mu_n} (P_a^* - P_n) + \min \left[0, \frac{q_w C_n^w}{\rho_w} \right]$$

where, as usual, W_i is a suitably chosen large number.

If there is a non-zero capillary pressure P_{cnw}, then equation (17) has the effect that no water phase will flow until the *NAPL* saturation becomes as small as possible. This is a numerical statement of the outlet effect [22]. In reservoir simulation, the outlet effect is negligible due to the large flow rates and large finite

difference cells. In contrast, the outlet effect is important in shallow groundwater systems.

Other boundary conditions can be simulated in a manner similar to equations (15-16).

6. Example With No Mass Transfer

The first example is the problem posed by Faust [2]. The model developed by Faust [2] does not have the ability to solve problems with mass transfer between phases, so all mass transfer terms in equations (8-9) are set equal to zero.

This problem consists of a porous medium $5m$ in depth and $16.9m$ in width. A constant absolute pressure $P_n = 131.85\ Kpa$ is specified on the bottom edge, with a constant recharge of $100 Kg/\text{year}/m^2$ of water on the surface. There is a point source of contaminant at the upper left corner of $900 Kg/\text{year}$. All other boundaries are no-flow. This problem was modelled on a 6×20 cell centered grid. A complete description of all physical properties is given in reference [2]. The thickness of the physical region was estimated to be $1m$ (this data was not mentioned in [2]). Constant rate source terms were used to simulate water and contaminant injection in the top cells, and a constant pressure sink term (as described in Section 5) was used to model the draining aquifer.

Two different cases were considered. One run used $\rho_n = 1200\ Kg/m^3$ ($\rho_w = 1000\ Kg/m^3$), and the other set $\rho_n = 950\ Kg/m^3$. Tabular values of the *NAPL* saturation with $\rho_n = 1200\ Kg/m^3$ at time $= 1.16$ years are given in Table 1, which can be compared with Table 5b of Faust [2]. The agreement between the two tables is good, except for the values for cell (20, 1). Faust [2] shows $S_n = 0.0$ for this cell, while the present model gives $S_n = .100$ (the critical saturation for the nonaqueous

phase). Clearly, the constant pressure boundary condition is simulated in a different way in the previous code [2]. The present model will require that the saturation is at least the critical value before any mass is removed from the system (see Section 5). Reduction of the timestep changed the results only in the third decimal place, while the material balance error for this run was less than 10^{-4}.

Table 2 gives the results for this same problem with $\rho_n = 950\ Kg/m^3$. This table can be compared with Table 5a from [2]. The agreement between the two models is quite good, especially for large saturation values. The difference between the two models is more pronounced for the small saturations near the leading edge of *NAPL*. This could be accounted for by the different method of discretizing the boundary conditions (as pointed out in the previous example with $\rho_n = 1200\ Kg/m^3$).

Reduction of the timestep did not change the results appreciably, and the material balance error for this run was less than 5×10^{-6}, indicating that the algebraic equations were being solved accurately. There was little difference between the fully implicit and adaptive implicit runs.

Table 3 shows run statistics for the case with $\rho_n = 1200\ Kg/m^3$. The average degree of implicitness is the average fraction of cells which are fully implicit during the course of the run. (A fully implicit run would have an average degree of implicitness $=1.0$, while an *IMPES* run would have an average degree of implicitness $=0.0$). For this simulation, the adaptive implicit run required an average degree of implicitness of only 16%. The adaptive implicit method required approximately 40% less CPU time than the fully implicit method. A larger saving in CPU time can be expected for larger problems, where the matrix solve begins to dominate.

Table 4 shows the statistics for the run with

$\rho_n = 950\ Kg/m^3$. Here, the average degree of implicitness was only 11% for the adaptive implicit run. Again, the adaptive implicit run required approximately 40% less CPU time than the fully implicit method.

In both cases, the fully implicit and adaptive implicit methods gave virtually the same results. Note that the total number of Newton iterations for the adaptive implicit method was approximately 25% higher than for the fully implicit technique. This is to be expected, since the change of state of some cells from *IMPES* to fully implicit during the course of a timestep will generally require more Newton iterations. The average degree of implicitness required is surprisingly low for both runs, even with some large timesteps (90 days) at the end of the runs.

7. Example With Mass Transfer

In order to demonstrate the variable substitution method for handling *NAPL* appearance and disappearance, an example run was carried out with non-zero air and water partition coefficients.

Figure 1 shows the domain of the problem. Water is injected along the top at a rate of 100 cm/year. A point source of contaminant ($1 m^3$/year) is placed on the left boundary $4m$ below the surface, and a constant pressure boundary with $P_n = 129.4\ Kpa$ is specified along the bottom edge.

A 13×10 cell centered discretization was used, with half cells on the boundaries, so that the centers of the boundary cells coincided exactly with the boundaries. The model was run to a simulated time of 3 years.

A constant pressure $P_n = 100\ Kpa$ air boundary is specified along the top edge (top row of cells). The recharge due to rainfall is modelled by injecting water along the top row of cells.

Consequently, the contaminant can leave the system by convection in the water phase through the bottom edge, and diffusion into the air at the top.

The physical properties and discretization data are given in Table 5a and 5b. The physical properties of the contaminant are assumed to be those of Toluene [7]. The relative permeability and capillary pressure data are those from the previous example [2].

Table 6 gives the run statistics for this problem and the identical run with $K_n^a = K_n^w = 0$. Note that the average degree of implicitness for the case with mass transfer is 85%, while the case with no mass transfer had an average degree of implicitness of 37%. This is because the stability criterion equation (A8) is dominated by the air diffusion condition at early times, and hence a large fraction of the cells turn implicit very quickly in the unsaturated zone. After the timesteps build up, the throughput condition for the dissolved contaminant in the water phase in the unsaturated zone is exceeded (recall that the stability conditions equation (A8) are used only if C_n^w is a primary variable).

The mass transfer simulation required approximately 40% more Newton iterations than the simulation with no mass transfer. Part of this difficulty was due to the diffusion upward of contaminant in the air phase. Equilibrium conditions then demanded that some of the diffused contaminant dissolve in the water phase, which was then convected downward due to gravity effects. Consequently, small amounts of contaminant were diffused upward and simultaneously convected downward. Not surprisingly, this created some difficulties for the Newton iteration.

The variable substitution method appeared to work well. Initially, S_n was identically zero everywhere, and remained zero in the saturated zone. As long as the amount of S_n appearing in a cell was reasonably large, then the Newton iteration proceeded quite smoothly through the phase appearance. Occasionally, if the

value of S_n was very small, the Newton iteration had some difficulty. This is because the mass of contaminant in the *NAPL* (proportional to S_n) was very small, as was the mass of contaminant in the water and air phases (also quite small since K_n^w and K_n^a are both small). Consequently, several Newton iterations were required to determine the precise state ($S_n = 0$ or $S_n \neq 0$) of the cell, even though the amount of mass involved was very small. This problem was cured by detecting this situation and underrelaxing the Newton iteration.

It can be seen from Table 6 that the simulation with mass transfer required almost twice as much CPU time as the simulation with no mass transfer. This is a result of the greater degree of implicitness and extra Newton iterations required for the case with mass transfer.

Figure 2 shows the *NAPL* saturation contours at three years. The *NAPL* has penetrated approximately $20m$ away from the source in the horizonal direction. Since the contaminant density is less than water, the maximum saturation occurs near the water saturated zone.

Figure 3 shows the normalized concentration (C_n^w/K_n^w) of contaminant in the water phase at three years. Since the concentration of contaminant in the air phase is proportional to the concentration in the water phase, the air phase concentration contours are similar and hence not shown.

It is interesting to see that a high level of contamination exists in the saturated water zone. This is due to the convective movement of water through the system. However, contamination also exists above the level of the pollutant source. This is due to diffusion in the air phase and subsequent dissolution in the water phase. This contamination persists in spite of the fact that there is a large throughput of water from the surface.

Table 7 shows the fate of injected fluids after three years. It is interesting to note that even though K_n^a is smaller than K_n^w, slightly more mass of contaminant escapes into the atmosphere than escapes into the aquifer. This is due to the large diffusion effect in the air phase, and is highly dependent on the value of the diffusion coefficent. The values used in this study were typical values used in references [7,8].

The results did not change significantly if smaller timesteps were used.

8. Conclusions

The adaptive implicit method worked well for three phase contamination problems with no inter-phase mass transfer. Savings of 40% in CPU time were obtained over fully implicit runs. For large problems, the matrix solve will begin to dominate. Since the solve will require work proportional to the square of the number of unknowns per cell, a larger saving for the adaptive implicit method can be expected for larger problems.

For simulations with mass transfer between phases, stability conditions required that most of the cells be solved using a fully implicit method. Of course, this is highly dependent on the air diffusion constant, and the magnitude of the water throughput. Consequently, problems involving mass transfer between phases are much more expensive to run than problems with no mass transfer.

The variable substitution technique provided a rigorous method of solving the flow and constraint equations for cells with S_n identically zero, and automatically switches to the correct formulation whenever the nonaqueous phase appears in a cell. This formulation gives a small material balance error even with relatively loose convergence tolerances. The variable substitution method also avoids some of the problems associated with having to specify initial conditions on nonexistent phases.

Finally, a complete description of the method for handling the boundary conditions by means of source/sink terms has been given. The precise method for specifying boundary conditions for shallow, multiphase flow systems has not been discussed in detail previously. In particular, it is important to pay careful attention to the outlet effect. This effect is negligible in petroleum reservoir simulation.

A1

Appendix

In this appendix, the stability condition for an *IMPES* type discretization of equations (8-9) is derived, assuming P_n^w, C_n^w are primary variables, with $S_n = 0$.

In order to simplify the algebra, equation (8) will be rewritten. Consider a finite different cell i, and define a face j of cell i as the interface between cell i and cell j. Then equation (8) can be written as:

$$\frac{V_{wi}^{N+1} - V_{wi}^{N}}{\Delta t} = \sum_j f_j^w \tag{A1}$$

where the volume of water in cell i is

$$V_{wi} = (\phi\, S_w)_i\, V_i$$

and defining the volumetric flow across face j of cell i as:

$$f_j^w = \frac{V_i}{\Delta_j}\, T_{wj+½}^{N}\, K_{j+½}\, \psi_{wj+½} \tag{A2}$$

where:

$$\Delta_j = \Delta x_i \qquad j-x \text{ direction}$$

$$= \Delta y_i \qquad j-y \text{ direction}$$

and $j+½$ refers to quantitites evaluated at the interface between cell i and cell j. ρ_w has been assumed constant.

Let:

$$V_{ai}^N = (\phi\ S_a)_i^N\ V_i \tag{A3}$$

$$\triangle_{j+\frac{1}{2}} = (\triangle_j + \triangle_{j+\frac{1}{2}})/2$$

$$D_j' = (\phi\ S_a\ D_n^a\ \xi_a)_{j+\frac{1}{2}}^N\ \frac{V_i}{\triangle_j}$$

Then assuming $S_{ni}^N = S_{nj}^N = 0$, $S_{ni}^{N+1} = S_{nj}^{N+1} = 0$, then equation (9) can be written as:

$$\frac{1}{\triangle t}\left[V_a^{N+1}\left(\frac{K_n^a}{K_n^w}\right)(C_{ni}^w)^{N+1} - V_a^N\left(\frac{K_n^a}{K_n^w}\right)(C_{ni}^w)^N \right. \tag{A4}$$

$$\left. + V_w^{N+1}\,(C_{ni}^w)^{N+1} - V_w^N\,(C_{ni}^w)^N \right]$$

$$= \sum_j \left\{ \max\,(f_j^w, 0)\ C_{nj}^{wN} \right.$$

$$\left. - |\min\,(0, f_j^w)\ |\ C_{ni}^{wN} \right\}$$

$$+ \sum_j D_j'\left(\frac{K_n^a}{K_n^w}\right)\left[\frac{C_{nj}^{wN} - C_{ni}^{wN}}{\triangle_{j+\frac{1}{2}}}\right] D_j'$$

Noting that:

$$V_{wi}^{N+1}\,(C_{ni}^{w})^{N+1} - V_{wi}^{N}\,(C_{ni}^{w})^{N} \tag{A5}$$

$$= V_{wi}^{N+1}\left[(C_{ni}^{w})^{N+1} - (C_{ni}^{w})^{N}\right]/\Delta t$$

$$+ (C_{ni}^{w})^{N}\left[V_{wi}^{N+1} - V_{wi}^{N}\right]/\Delta t$$

$$= V_{wi}^{N+1}\,(C_{ni}^{w})^{N+1} - (C_{ni}^{w})^{N}\Big]/\Delta t$$

$$+ (C_{n}^{w})_{i}^{N}\left\{\sum_{j}\left\{\max(f_{i}^{w}, 0)\right.\right.$$

$$\left.\left. - |\min\,(f_{i}^{w}, 0)|\right\}\right]$$

where equation (A1) has been used in the last step above. Finally, equation (A4) takes the form:

$$\frac{1}{\Delta t}\left\{\left(\frac{K_{n}^{a}}{K_{n}^{w}}\right)\left[V_{ai}^{N+1}\,(C_{ni}^{w})^{N+1} - V_{ai}^{N}\,(C_{ni}^{w})^{N}\right]\right. \tag{A6}$$

$$\left. + V_{wi}^{N+1}\left[(C_{ni}^{w})^{N+1} - (C_{ni}^{w})^{N}\right]\right\}$$

$$= \sum_{j}\max\,(f_{j}^{w}, 0)\,(C_{nj}^{wn} - C_{ni}^{wN})$$

$$+ \sum_{j}\left(\frac{K_{n}^{a}}{K_{n}^{w}}\right)\left[\frac{C_{nj}^{wN} - C_{ni}^{wN}}{\Delta_{j+1/2}}\right] D_{j}'$$

Equation (A6) can be rearranged in the form:

$$(C_{ni}^{W})^{N+1} = g\ (C_{nj}^{wN},\ C_{ni}^{wN})$$

Note that:

$$g(0, 0) = 0$$

$$g(C^*, C^*) = C^*\beta$$

$$\beta = \frac{[V_{ai}^{N} \left(\frac{K_n^a}{K_n^w}\right) + V_{wi}^{N+1}]}{[V_{ai}^{N+1} \left(\frac{K_n^a}{K_n^w}\right) + V_{wi}^{N+1}]} \tag{A7}$$

It is easy to see that:

$$\frac{\partial g}{\partial C_{nj}^{wN}} > 0$$

and that:

$$\frac{\partial g}{\partial C_{ni}^{wN}} > 0$$

if the following condition is satisfied:

$$\Delta t\ \frac{\left(\sum_j [\max(f_i, 0) + \left(\frac{K_n^a}{K_n^w}\right) \frac{D_j'}{\Delta_{j+\frac{1}{2}}}]\right)}{\left(V_{ai}^{N} \left(\frac{K_n^a}{K_n^w}\right) + V_{wi}^{N+1}\right)} < 1 \tag{A8}$$

Equations (A7-A8) imply that:

$$0 < (C_{ni}^{w})^{N+1} < \max\,(C_{ni}^{wN})\ \ \beta$$

if:

$$\forall_i, \qquad 0 < C_{ni}^{wN} < \max\,(C_{ni}^{wN}) \tag{A9}$$

Note that β is not necessarily one. To examine the physical reason for this, let $V_{wi}^{N+1}=0$, then:

$$\beta = \frac{V_{ai}^{N}}{V_{ai}^{N+1}}$$

so that if the air phase volume decreases, then $(C_{ni}^{w})^{N+1}$ will be larger than max (C_{ni}^{wN}). This is because the convective motion of the air phase has been ignored in equations (1-2). Also, $(C_{ni}^{w})^{N+1}$ cannot become larger than K_n^w, since this triggers the appearance of the nonaqueous phase (see equation (14)). Consequently, equation (9) is numerically stable if $S_{ni}^{N} = S_{ni}^{N+1} = 0$, and condition (A8) is satisfied.

References

[1] Peaceman, D.W., **Fundamentals of Numerical Reservoir Simulation,** Elsevier, New York, 1977.

[2] Faust, C.R., "Transport of immiscible fluids within and below the unsaturated zone: a numerical model", Water Resour Res. **21** (1985) 587-596.

[3] Osbourne, M, and J. Sykes, "Numerical modelling of immiscible organic transport of the Hyde Park landfill", Water Resour Res. **22** (1986) 25-33.

[4] Abriola, L.M. and G.F. Pinder, "A multiphase approach to the modelling of porous media contamination by organic compounds 1. Equation development", Water Resour Res. **21** (1985) 11-18.

[5] Abriola, L.M. and G.F. Pinder, "A multiphase approach to the modelling of porous media contamination by organic compounds 2. Numerical simulation", Water Resour Res. **21** 19-26.

[6] Pinder, G.F. and L.M. Abriola, "On the simulation of nonaqueous phase organic compounds in the subsurface", Water Resour Res. **22** (1986) 1095-1195.

[7] Corapcioglu, M.Y. and A.L. Baehr, "A compositional multiphase model for groundwater contamination by petroleum products 1. Theoretical considerations", Water Resour Res. **23** (1987) 191-200.

[8] Baehr, A.L. and M.Y. Corapcioglu, "A compositional multiphase model for groundwater contamination by petroleum products 2. Numerical solution", Water Resour Res. **23** (1987) 201-213.

[9] Forsyth, P.A. and P.H. Sammon, "Practical considerations for adaptive implicit methods in reservoir simulation", J.

Comp. Phys. **62** (1986) 265-281.

[10] Forsyth, P.A. "Comparison of single phase and two phase numerical model formulation for saturated-unsaturated groundwater flow", (submitted to Comp. Meth. Appl. Mech. Eng.) 1987.

[11] Dake, L.P., **Fundamentals of Reservoir Engineering,** Elsevier, New York, 1978.

[12] Stone, H.L., "Estimation of three phase relative permeability and residual oil data", J. Can .Pet. Tech. **12** (1973) 53-61.

[13] Aziz, K. and A. Settari, **Petroeum Reservoir Simulation,** Applied Science, London, 1979.

[14] Forsyth, P.A. and P.H. Sammon, "Quadratic convergence for cell centered grids", (to appear, Appl. Num. Math) 1987.

[15] Thomas, G.W. and D.H. Thurnau, "Reservoir simulation using an adaptive implicit method", Soc. Pet. Eng. J. **23** (1983) 760-768.

[16] Forsyth, P.A. and P.H. Sammon, "Gas phase appearance and disappearance in fully implicit black oil simulation", Soc. Pet. Eng. J. **24** (1984) 505-507.

[17] Behie, A. and P.K.W. Vinsome, "Block iterative methods for fully implicit reservoir simulation" Soc. Pet. Eng. J. **22** (1982) 659-658.

[18] Wallis, J.R., "Incomplete gaussian elimination as a preconditioning for generalized conjugate gradient acceleration", Seventh SPE Symposium on Reservoir Simulation, San Francisco, 1983.

[19] Behie, A. and P.A. Forsyth, "Incomplete factorization methods for fully implicit simulation of enhanced oil recovery", SIAM J. Sci. Stat. Comp. **5** (1984) 543-561.

[20] Sammon, P.H., "An analysis of upstream differencing", (submitted to Soc. Pet. Eng. J.) 1985.

[21] Forsyth, P.A., "Adaptive implicit criteria for two phase flow with gravity and capillary pressure", (submitted to SIAM.J. Sci. Stat. Comp.)

[22] Settari, A., 'Numerical simulation of three phase coning in petroleum reservoirs", Ph.D. thesis, University of Calgary, 1973.

TABLE 1

Computed saturations of nonaqueous phase for example from Faust [2]. Density of nonaqueous phase 1200 Kg/m^3. Time =1.16 years.

Column

Row	1	2
1	.178	.105
2	.175	.100
3	.169	.095
4	.163	.091
5	.157	.085
6	.139	.075
7	.123	.069
8	.122	.068
9	.122	.067
10	.122	.064
11	.122	.064
12	.122	.063
13	.122	.062
14	.121	.061
15	.121	.059
16	.121	.058
17	.121	.057
18	.121	.056
19	.119	.052
20	.100	0.0

0.0 at all other cells.

TABLE 2

Computed saturation of nonaqueous phase for example from Faust [2]. Density of nonaqueous phase 950 Kg/m^3. Time =1.07 years.

	Column				
Row	1	2	3	4	5
1	.378	.371	.364	.324	.121
2	.396	.390	.383	.264	.056
3	.414	.410	.348	.203	.019
4	.433	.387	.287	.135	0.0
5	.381	.325	.223	.056	0.0
6	.315	.261	.156	.015	0.0
7	.242	.186	.092	0.0	0.0
8	.150	.101	.006	0.0	0.0
9	.059	.004	0.0	0.0	0.0

0.0 at all other cells

TABLE 3

Statistics for example from Faust [2], density of nonaqueous phase 1200 Kg/m^3.

	Fully Implicit	Adaptive Implicit
Total Timesteps	12	12
Total Newton Iterations	96	104
Average Implicitness	1.0	.16
Total CPU time (VAX 11/780 Seconds)	183	114
Material Balance Error	1×10^{-4}	1×10^{-4}

TABLE 4

Statistics for example from Faust [2], density of nonaqueous phase 950 Kg/m^3.

	Fully Implicit	Adaptive Implicit
Total Timesteps	9	9
Total Newton Iterations	46	55
Average Implicitness	1.0	.11
Total CPU time (VAX 11/780 Seconds)	98	63
Material Balance Error	4×10^{-6}	1×10^{-6}

TABLE 5a

Data for example with mass transfer.

Permeability	$10^{-12}\ m^2$
Porosity	.3
Viscosity water	$.001\ Kg\ m^{-1}\ S^{-1}$
Viscosity NAPL	$.001\ Kg\ m^{-1}\ S^{-1}$
Density, water	$1000\ Kg/m^3$
Density, NAPL	$862\tilde{}Kg/m^3$
NAPL-water partition coefficient K_n^w	$.515\ Kg/m^3$
NAPL-air partition coefficient K_n^a	$.133\ Kg/m^3$
NAPL air diffusion constant D_n^a	$10^{-5}\ m^2/\text{sec}$
Air phase tortuosity factor ξ_a	.2
Grid Data (13×10)	
$\triangle z$	$1m$
$\triangle x$	$1, 1.5, 2, 3, 4, 6, 8, 10, 10, 10m$
$\triangle y$	$1m$

TABLE 5b

Data for example with mass transfer.

Initial Conditions

Depth	S_w	P_n (Kpa)
0.0	.2	22.9
1.0	.2	22.9
2.0	.3	31.3
3.0	.4	41.1
4.0	.5	51.0
5.0	.6	60.8
6.0	.7	70.6
7.0	.8	80.4
8.0	.9	90.2
9.0	1.0	100.0
10.0	1.0	109.8
11.0	1.0	119.6
12.0	1.0	129.4

Relative permeability and capillary pressure from Table 4, Faust [2]. Nonaqueous phase saturation $S_n = 0$ everywhere initially.

TABLE 6

Run statistics for the example with mass transfer. Simulated time =3 years.

	Mass Transfer	No Mass Transfer $K_n^a=0$, $K_n^w=0$
Total timesteps (repeats)	19 (1)	18 (0)
Average implicitness	.85	.37
Total CPU time (VAX 11/780 seconds)	308	146
Material balance error	3×10^{-6}	5×10^{-5}

TABLE 7

Fate of injected and produced fluids for the simulation with mass transfer.

	Nonaqueous phase contaminant (m^3)	Water (m^3)
Total injected	3.0	151.5
Total escaping into draining aquifier	9.6×10^{-3}	148.7
Total escaping into atmosphere	1.2×10^{-2}	0.0

Figure Captions

(1) Domain for problem with inter-phase mass transfer.

(2) Non-aqueous phase saturation contours at three years.

(3) Normalized concentration of contaminant in the water phase (maximum = 1.0) at three years.

FIGURE 1

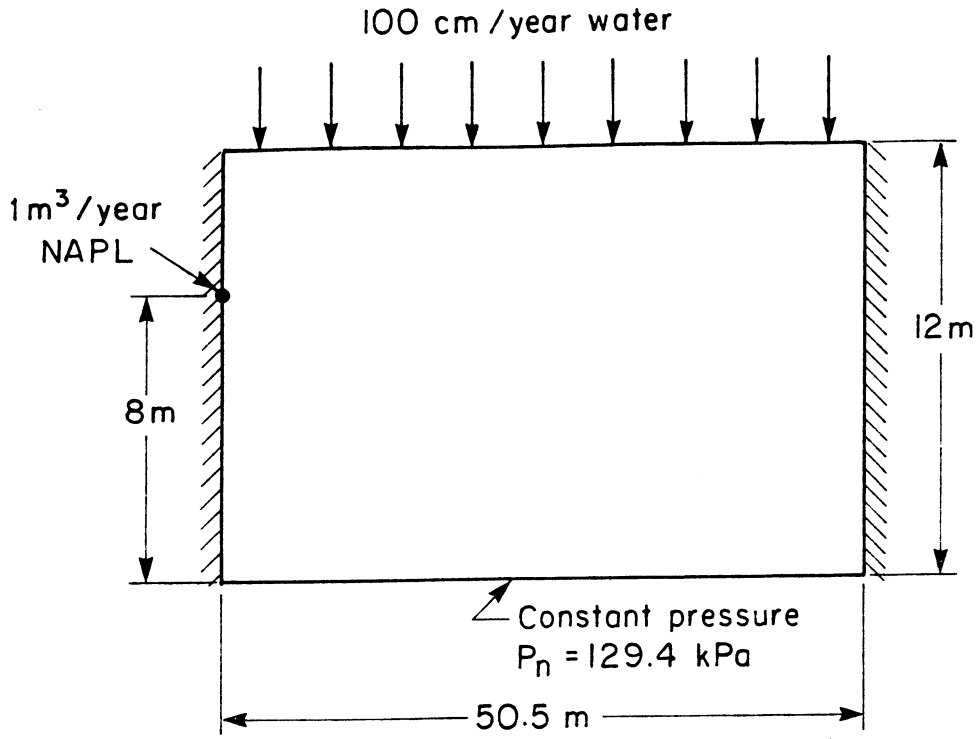

(1) Domain for problem with inter-phase mass transfer.

FIGURE 2

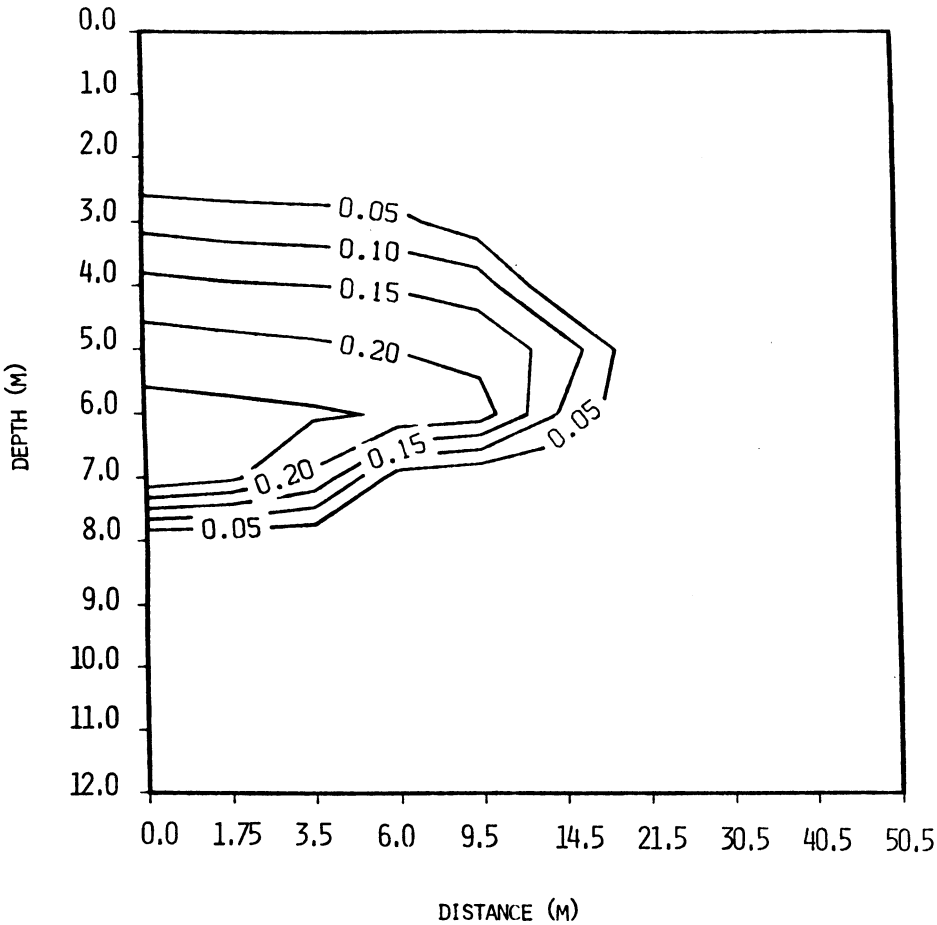

(2) Non-aqueous phase saturation contours at three years.

FIGURE 3

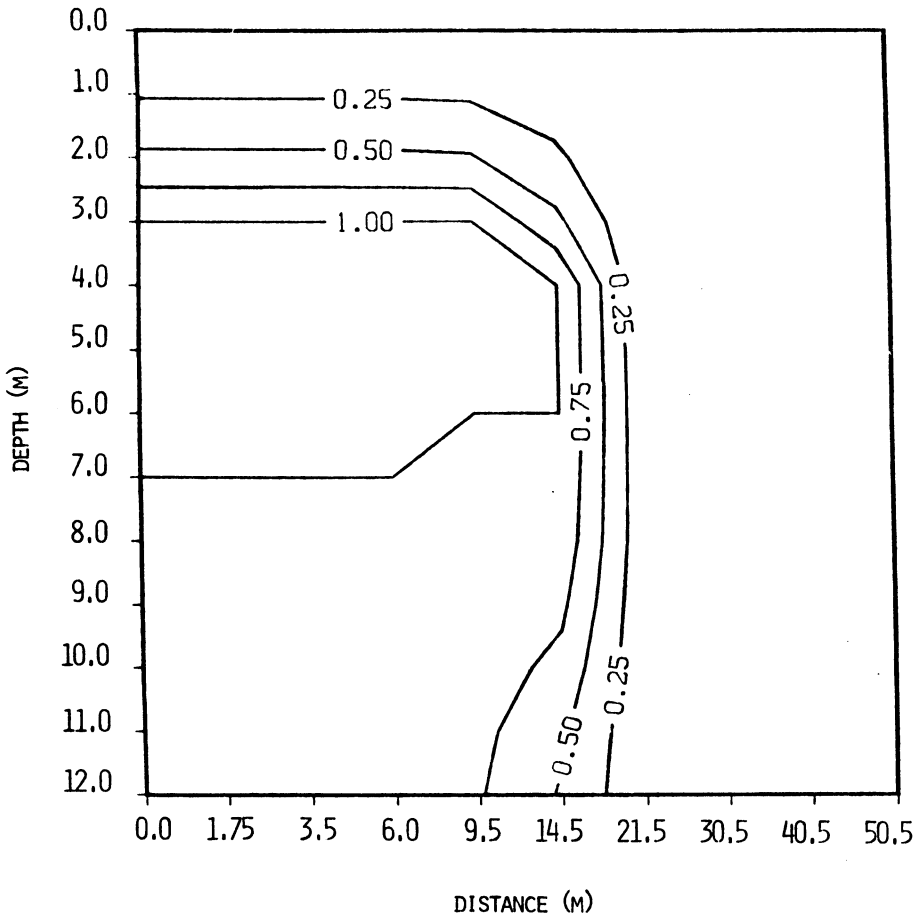

(3) Normalized concentration of contaminant in the water phase (maximum = 1.0) at three years.